Investigating Age Invariant Face Recognition Based on Periocular Biometrics

Felix Juefei-Xu*[1], Khoa Luu*[1,2], Marios Savvides[1], Tien D. Bui[2], and Ching Y. Suen[2]

[1]CyLab Biometrics Center, Carnegie Mellon University, Pittsburgh, Pennsylvania, USA

felixu@cmu.edu, msavvid@ri.cmu.edu

[2]CENPARMI, Concordia University, Montréal, Québec, Canada

{kh_lu,bui,suen}@encs.concordia.ca

Abstract

In this paper, we will present a novel framework of utilizing periocular region for age invariant face recognition. To obtain age invariant features, we first perform preprocessing schemes, such as pose correction, illumination and periocular region normalization. And then we apply robust Walsh-Hadamard transform encoded local binary patterns (WLBP) on preprocessed periocular region only. We find the WLBP feature on periocular region maintains consistency of the same individual across ages. Finally, we use unsupervised discriminant projection (UDP) to build subspaces on WLBP featured periocular images and gain 100% rank-1 identification rate and 98% verification rate at 0.1% false accept rate on the entire FG-NET database. Compared to published results, our proposed approach yields the best recognition and identification results.

1. Introduction

The research in age-related face recognition has gained lots of prominence lately due to the challenging problems of human face aging processes and strong demand of robust face recognition system across ages. Such face recognition systems are crucial in practical applications that need the compensation of age, *e.g*. missing children identification or passport verification, where there is a significant age difference between probe and gallery images.

However, compared to the state-of-the-art results of stand-alone face recognition systems, the precision of current age invariant face recognition systems is still very limited due to the lack of robustly identifiable features that are stable across ages. Additionally, face aging databases are usually collected from scanned images in different poses, illumination and expression as in Figure 2. These corpora themselves challenge not only age-related studies but also other face-related problems, *e.g*. illumination and pose correction, expression recognition. Therefore, proposed age invariant features that work on these databases also have to be robust against the variations in illumination, poses and facial expressions.

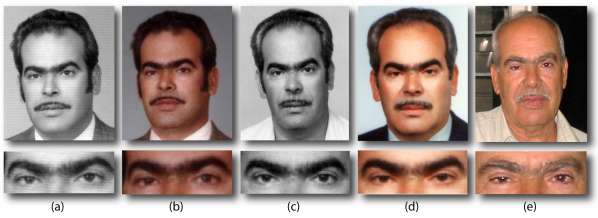

Figure 1. Examples of an aging subject from FG-NET. (a) Age 31, (b) Age 40, (c) Age 46, (d) Age 61, (e) Age 69. Periocular region is perceptually more stable across ages than the full face.

1.1. Motivation

Although holistic model based approaches have been applied efficiently in age invariant face recognition (Section 2.1), they still have some drawbacks. First, as discussed previously, the available face aging databases are usually collected from scanned images in different poses, illumination and expression. Meanwhile most face modeling methods require having face images with frontal pose, normal illumination and neutral expression to get the best fit results. Additionally, in order to have an exact model to represent the aging process, systems have to use a huge number of training images that are usually inefficient for the currently limited face aging databases. Second, forensic scientists proved that human face aging strongly depends on ethnicity and genders [20]. Although human faces have the same general manner when aging, each ethnic and gender group has distinct characteristics in face aging. Therefore, it is insufficient to assume that similar faces age in similar ways for each and every individual.

*These authors contributed equally to this work and should be considered co-first authors.

978-1-4577-1359-0/11/$26.00 ©2011 IEEE

In order to overcome these limitations, we propose to use periocular, the most age invariant facial region, to extract discriminative local features that are distinct for every subject. Compared to the global feature based approaches, the local features inherently possess spatial locality and orientation selectivity. These properties allow the local feature representations to be robust to aging, illumination, and expression variations. Considering that the entire face with high structural complexity easily changes over time in terms of color, texture and structure. That is why full face modeling for age invariance is difficult. Periocular region, however, changes rather little over time because the shape and location of eyes remain largely unchanged while the mouth, nose, chin, cheek, *etc*., are more susceptible to changes given a loosened skin [15]. Additionally, periocular region has the most dense and the most complex biomedical features on human face, *e.g*. contour, eyelids, eyeball, eyebrow, *etc*., which could all vary in shape, size and color. Biologically and genetically speaking, more complex structure means more "coding processing" going on with fetal development, and therefore more proteins and genes involved in the determination of appearance. That is why periocular region should be the most important facial area for distinguishing people. With stability across ages and strong discriminative power, using periocular region for age invariant face recognition is by all means rational and wise.

Prior work on age-related face recognition will be discussed in Section 2. We will introduce our proposed approach in Section 3 with preprocessing schemes and unsupervised discriminant projection (UDP) as subspace modeling technique, and followed by details on Walsh-Hadamard transform encoded local binary patterns (WLBP) in Section 4. Experiments setup and results will be shown in Section 5. The proposed approach is able to reach 100% rank-1 identification rate and 98% verification rate at 0.1% false accept rate with leave-one-person-out (LOPO) strategy on entire FG-NET database and provides significant improvement over the best performing algorithm by far. Finally, we will conclude our work in Section 6.

2. Prior Work

The research in age related face recognition has increased since 2002. However, related published work is still very limited in both quantity and quality. Indeed, most proposed approaches dealing with face aging are mainly focusing on either face age progression simulation [19] or age estimation [4, 5, 7]. One of the first papers related to face aging from digital images belongs to Kwon *et al*. (1993) [11]. They used 47 high resolution images of a face to classify the images into one of three age groups: babies, young adults or senior ones. Their approach was based on geometric ratios of key face features and wrinkle analysis. However, their database was limited to 47 high resolution photos and such ideal image quality would be very difficult to acquire in practical applications.

Figure 2. First row shows examples from FG-NET with illumination variation due to different illumination condition. Second row shows corresponding illumination preprocessing results.

Generally, recent proposed age related face recognition methods can be divided into two categories: local approaches and holistic approaches. In this section, we will review some prior studies on both approaches.

2.1. Global Approaches for Age Invariant Face Recognition

Most holistic approaches try to generate face aging models and build aging functions to simulate or compensate for the aging process. Lanitis *et al*. [12] used the active appearance models (AAM) [2], a statistical face model, to study age estimation problems. In their approach, after AAM parameters were extracted from face images landmarked with 68 points, an aging function was built using Genetic Algorithms to optimize the aging function. Sethuram *et al*. [19] also built a high accuracy face aging model based on AAMs, support vector machines (SVMs) and Monte-Carlo simulation. In their paper, two experiments were setup. In experiment 1, they proved that the accuracy of face recognition goes down when probe faces age. In experiment 2, the probe faces are first artificially aged to the same age of the gallery by using the face aging model. Then, the face recognition algorithm is applied to get a higher accuracy than the ones in experiment 1. Meanwhile Geng *et al*. [5] introduced an AGing pattErn Subspace (AGES) on the assumption that similar faces age in similar ways for all individuals. Their basic idea is to model the aging pattern, which is defined as a sequence of a particular individual's face images sorted in time order, by constructing a representative subspace. The proper aging pattern for a previously unseen face image is determined by the projection in the subspace that can reconstruct the face image with a minimum reconstruction error, while the position of the face image in that aging pattern will then indicate its age. Mahalingam *et al*. [14] proposed to use a graph based face representation that contains facial geometry and appearance for their age invariant face recognition system. The probabilistic aging model is individually

setup by using Gaussian mixture models (GMMs). In the graph construction algorithm, the feature points of an image and their descriptors are used as vertices and labels correspondingly. There are two steps in their matching process. First, the search space is reduced and the potential individuals are identified effectively by using a maximum a posterior (MAP) for each individual based aging model. Second, a simple deterministic graph matching algorithm is used to exploit the spatial similarity between the graphs. Park *et al*. [17] presented an approach to age invariant face recognition by using a 3D generative model for face aging. In their method, in order to compensate for the age effect, probe face images are first transformed to the same age as the gallery image by using the trained 3D aging model. Then, FaceVACS, a commercial face recognition engine, was used to evaluate the identification results. Some of the reviewed methods will be summarized and compared with our proposed approach in the Table 2.

2.2. Local Approaches for Age Invariant Face Recognition

The local based approaches for age invariant face recognition have not been well explored. Contrary to holistic face interpretation, most of these local feature based methods are proposed to solve the age estimation problem thanks to the sufficiency of local patches to overcome the shortcomings of sensitivity, illumination variations and image occlusions. Moreover, age features are usually encoded by local information *e.g*. wrinkles on the forehead or at the eye corners. Li *et al*. [13] introduced an advanced algorithm for face recognition against age invariant using multi-feature discriminant analysis (MFDA), which combines scale invariant feature transform (SIFT) and multi-scale local binary patterns (MLBP), to encode the local features. Yan *et al*. [21] introduced a method using coordinate patches and GMMs to estimate facial ages. In their method, face image of an individual is encoded as an ensemble of overlapped spatially flexible patches (SFPs), each of which integrates coordinate information together with the local features that are extracted by 2D discrete cosine transform (DCT). These extracted SFPs are modeled with GMMs to estimate the age of a person in the input facial image, by comparing the sum of likelihoods from total SFPs of the hypothetic age. Guo *et al*. [7] introduced an age estimation method by using a manifold learning scheme. He designed a local based regression classifier to learn the aging function and use it to predict the age from a given image. Fu *et al*. [4] also proposed a manifold learning technique in which a low dimensional manifold is learn from a set of age separated face images. Linear and quadratic regression functions were applied on the low dimensional feature vectors from the respective manifolds in face age estimation. Drygajlo *et al*. [3] presented an approach to perform face verification across age progression by using a Q-stack classifier.

3. Our Proposed Approach

In this section, we will detail our proposed approach. In order to obtain age invariant features, we first perform preprocessing schemes, such as pose correction, illumination and periocular region normalization, and then apply robust WLBP on periocular region only. Finally, we use UDP to build subspaces on WLBP featured periocular images.

3.1. Database

We perform our experiments on a public aging database FG-NET containing 1,002 high resolution color or gray scale face images of 82 subjects from multiple race with large variation of lighting, expression, and pose. The image size is approximately 400×500 in pixels. The age range is from 0 to 69 years (on average, 12 images per subject).

3.2. Pose Correction

Pose correction is a key preprocessing step in order to generate good results using AAM. As in Figure 3, the facial poses (column (e)) have been corrected from the given faces (column (a)). The transform $\mathbf{T}$, usually known as a pose correction that rotates the point $p(x, y)$ by θ, scales by s and translates by (x_T, y_T), and is constructed as:

$$\mathbf{T}\begin{pmatrix} x \\ y \end{pmatrix} = \begin{pmatrix} x_T \\ y_T \end{pmatrix} + \begin{pmatrix} s \cdot \cos\theta & s \cdot \sin\theta \\ -s \cdot \sin\theta & s \cdot \cos\theta \end{pmatrix} \begin{pmatrix} x \\ y \end{pmatrix} \quad (1)$$

3.3. Illumination Normalization

In FG-NET database, photos are taken under various illumination conditions. Illumination is the most significant factor affecting face appearance besides pose variation. The anisotropic diffusion model [6] has demonstrated excellent performance in challenging illumination conditions. Unfortunately, this algorithm is computationally demanding. To speed up the process, we follow a parallelized implementation of the anisotropic diffusion image preprocessing algorithm running on GPUs programmed with nVidia's CUDA framework and results are shown in Figure 2.

3.4. Periocular Region Normalization

The FG-NET database has severe pose variation. In order to localize the periocular region on images without pose correction, we utilize the 68 facial landmark points that are given in FG-NET to locate the eyes, and then rotation and eye coordinate normalization are performed to horizontally align left and right eyes with fixed eye coordinates for every image. On images with pose correction, since the faces are already well aligned, simple crop is sufficient. After periocular region normalization, the entire strip containing both

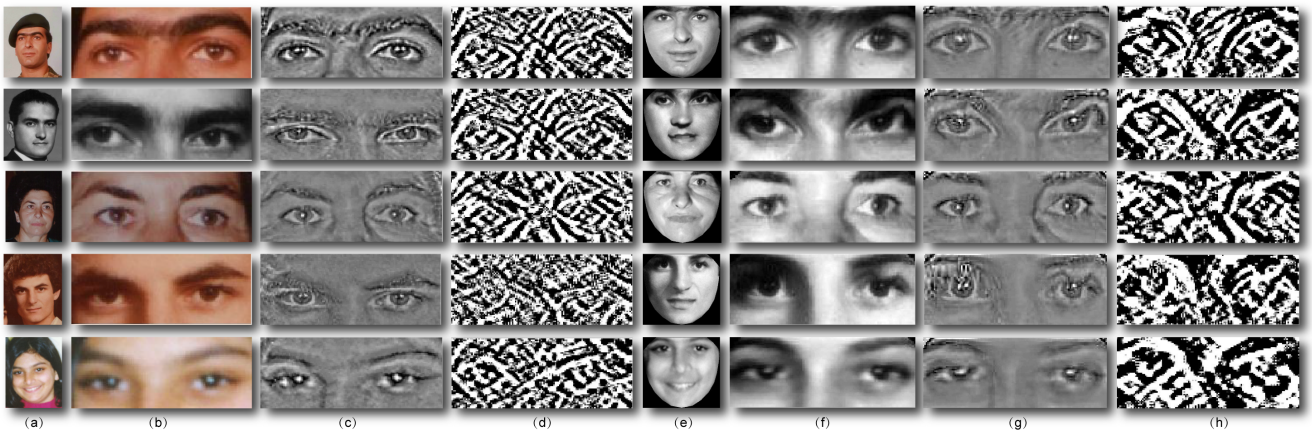

Figure 3. (a) original input full face image with pose and illumination variation, (b) normalized periocular region from original input, (c) illumination preprocessing, (d) WLBP featured periocular image, (e) full face after pose correction, (f) normalized periocular region after pose correction, (g) illumination preprocessing after pose correction, (h) WLBP featured periocular image after pose correction.

eyes is cropped in size of 50×128. Figure 1 shows examples of periocular region normalization on images without pose correction.

3.5. Feature Extraction Technique

We propose to use WLBP, an variant of LBP, as feature extractor to capture the locally discriminative characteristics on periocular region for age invariant face recognition. Details of WLBP will be discussed in Section 4.

3.6. Unsupervised Discriminant Projection

Unsupervised discriminant projection (UDP) [22] has been used in various applications where it has demonstrated efficacy against PCA, LDA, LPP and some common manifold techniques to find a optimal subspace. Compared to principal component analysis (PCA) that simply learns global information and locality preserving projections (LPP) [8] that only considers the local information, UDP has ability to comprise both local and non-local information. Instead of using the within-class and between-class scatter matrices as in linear discriminant analysis (LDA), UDP tries to find a optimal projection that minimizes the local scatter matrix S_L and maximizes the non-local scatter matrix S_N concurrently. Additionally, contrary to LDA, UDP is an unsupervised classification method where the training labels are not taken into account.

Given a training set in C classes with N labeled items $x_1, \ldots, x_N$ where $x_i \in \Re^d$, the objective function for UDP is defined as in Eqn. 2:

$$w* = \arg\max \frac{w^T S_N w}{w^T S_L w} \tag{2}$$

where S_L is the local scatter covariant matrix

$$S_L = \frac{1}{2} \sum_{i=1}^{N} \sum_{j=1}^{N} \mathbf{A}_{ij} (x_i - x_j)(x_i - x_j)^T \tag{3}$$

and S_N is the non-local scatter covariant matrix

$$S_N = \frac{1}{2} \sum_{i=1}^{N} \sum_{j=1}^{N} (1 - \mathbf{A}_{ij})(x_i - x_j)(x_i - x_j)^T \tag{4}$$

$\mathbf{A}$ is an adjacency matrix that is produced by K-nearest neighbors (KNN) method.

$$\mathbf{A}_{ij} = \begin{cases} 1 & \text{if } x_i, x_j \text{ are mutually KNN} \\ 0 & \text{otherwise} \end{cases} \tag{5}$$

Eqn. 2 can be solved by the eigen problem: $S_N w = \lambda S_L w$.

4. Walsh-Hadamard Transform Encoded LBP

The basic idea of LBP approach [16] is that all neighbors with values greater than that of the center pixel are assigned value 1 and 0 otherwise. The 8 binary numbers associate with the 8 neighbors are then read sequentially to form an 8-bit binary string in the case of 3×3 kernel. The equivalent of this binary string (usually converted to decimal) may be assigned to the center pixel as the local texture.

In addition to directly applying LBP on raw pixel for feature extraction, it's intuitively reasonable to post-apply LBP upon other feature extraction techniques.

Here we introduce Walsh-Hadamard transform encoded local binary patterns (WLBP) which is the fusion of Walsh-Hadamard transform and LBP. In order to speed up the transform, we use Walsh masks as convolution filters to approximate the Walsh-Hadamard transform.

Convolution filters such as Walsh masks [1, 18] can capture local image characteristics. The Walsh functions could

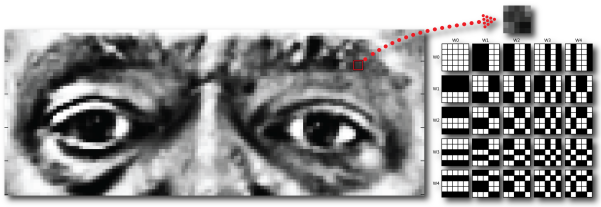

Figure 4. Example of applying Walsh masks. Expand each 5×5 kernels (right) using 25 Walsh basis images. The coefficients are treated as features assigned to the center pixel.

be used to construct a complete and orthonormal basis in terms of which any matrix of a certain size may be expanded. In the case of a 5×5 local kernel, the Walsh filters must correspond to the 5 sample long discrete versions of the Walsh function. Each set of these filters expands the 5×5 image patch in terms of a complete basis of elementary images. The Walsh function:

$$W_{2j+q}(t) = (-1)^{\lfloor \frac{2}{j} \rfloor + q}[W_j(2t) + (-1)^{j+q} W_j(2t-1)], \tag{6}$$

where $\lfloor \frac{2}{j} \rfloor$ means the integer part of $j/2$, q is either 0 or 1. We then sample each function at the integer points only, so we produce the following vectors for size 5:

$$\begin{cases} W_0^T = (1,1,1,1,1) \\ W_1^T = (-1,-1,-1,1,1) \\ W_2^T = (-1,-1,1,1,-1) \\ W_3^T = (1,1,-1,1,-1) \\ W_4^T = (1,-1,1,1,-1) \end{cases}$$

All possible combinations of Walsh vectors can be used to produce 25 2D basis images as shown in Figure 4. We can represent an image patch in terms of Walsh elementary functions of even size:

$$g = WfW^T, \tag{7}$$

where the transformation matrix W, the input image patch f and the output coefficients g are all of the same size, $N \times N$ (N is even). An even size transformation matrix constructed from Walsh functions is orthogonal thus its inverse is its transpose ($W^{-1} = W^T$).

In our experiment, we use image kernel of odd size such as 3×3, 5×5 and 7×7. As mentioned before, odd-sized Walsh vectors yield an odd-sized Walsh transformation matrix. Such matrix is no longer orthogonal ($W^{-1} \neq W^T$). In order to invert Eqn. 7, we make use of the inverse of W. Then we shall have [18] $W^{-1}g(W^T)^{-1} = f$.

So, we may use the inverse of matrix W to process the image. Then we have $g = (W^{-1})^T f W^{-1}$.

Once we have the Walsh coefficients, we apply LBP upon those coefficients and create WLBP. WLBP feature can dramatically improve the verification rate than LBP especially on periocular region [9, 10]. Examples of WLBP feature on periocular image are shown in Figure 3.

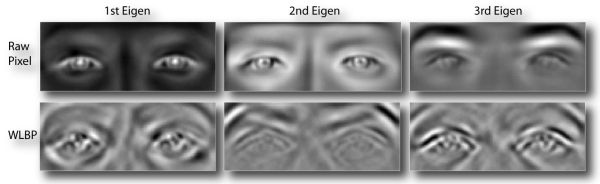

Figure 5. Top 3 eigenfaces from both raw pixel and WLBP feature.

5. Experimental Results

In this section, experimental setup is introduced and results reported with more quantitative analysis.

5.1. Setup

We conduct our evaluation experiments on entire FG-NET database which contains 1,002 uncontrolled images from 82 subjects (ages from 0 to 69) with pose and illumination variations. We conduct experiments by applying robust feature extraction technique, WLBP, on periocular region only on the entire FG-NET database and build subspaces using PCA, LPP [8], and UDP [22].

We follow the same leave-one-person-out (LOPO) scheme adopted by Li *et al.* [13] and Park *et al.* [17] (most commonly used in FG-NET evaluation) to separate the training and testing data. For LOPO scheme, all images of a single subject are used for testing and the remaining images for training. This is done for all subjects so that each subject is used for testing only once. This evaluation scheme makes sure that images from one subject are not in the testing and training set at the same time, so that the classifier cannot learn "within-class" relations.

The traditional method to build subspaces, *e.g.* in PCA, is to train directly on raw pixel intensity of the images. Our novel subspace representation yields significant improvement in recognition because we input featured images as shown in Figure 3 rather than raw pixel intensity for subspace modeling. Examples of top 3 eigenfaces from PCA using both raw pixel intensity and our robust WLBP featured images are shown is Figure 5.

Normalized cosine distance measurement is adopted to compute similarity matrix. The rank-1 identification rate and cumulative match characteristic (CMC) curves, verification rate (VR) at 0.1% false accept rate (FAR), equal error rate (EER) and receiver operating characteristic (ROC) curves of each evaluation method are analyzed.

5.2. Results

We perform evaluation experiments on the entire FG-NET database using subspace representations mentioned in Section 5.1 on featured periocular image using feature extraction technique from Section 4 following LOPO scheme. First, the experiments are performed on periocular crop with

Table 1. VR at 0.1% FAR, EER and rank-1 identification rate for FG-NET evaluation.

	PCA			***LPP***			***UDP***		
	VR	***EER***	***Rank-1***	***VR***	***EER***	***Rank-1***	***VR***	***EER***	***Rank-1***
Raw pixel	8.3%	42.9%	22.3%	8.9%	38.2%	8.9%	11.5%	27.2%	65.1%
WLBP	14.4%	40.4%	46.3%	40.2%	7.7%	85.1%	29.3%	15.9%	79.7%
Raw pixel with pose correction	9.0%	39.9%	27.0%	11.4%	27.5%	25.8%	49.6%	10.6%	97.4%
WLBP with pose correction	18.6%	31.0%	59.3%	92.8%	1.1%	99.5%	98.0%	0.6%	100%

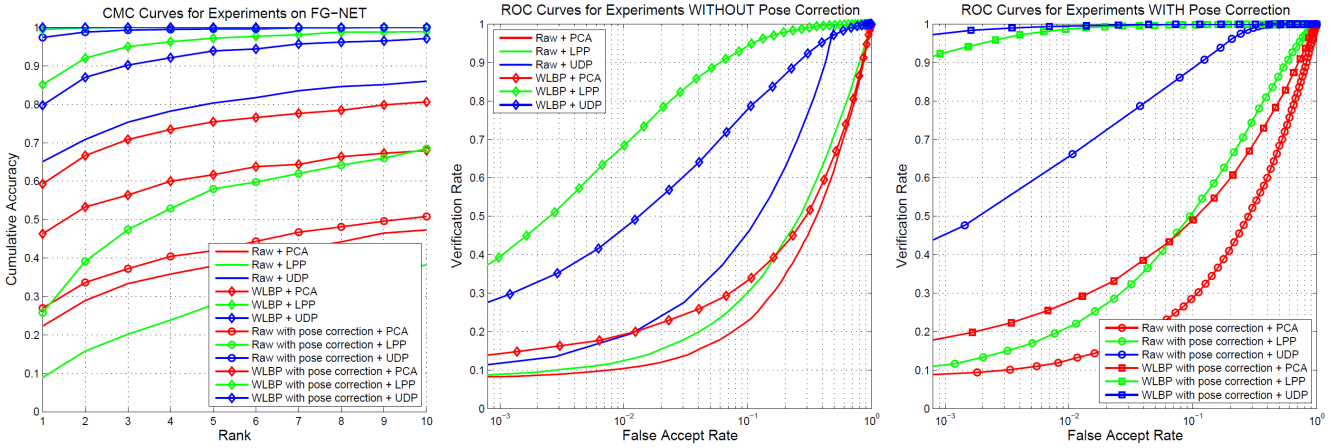

Figure 6. CMC curves (left), ROC curves without pose correction (middle), and with pose correction on FG-NET (right)

both raw pixel intensity and WLBP featured images without pose correction. Second, with pose correction using AAM.

First two rows in Table 1 are corresponding to experiments without pose correction and last two rows with pose correction. VR at 0.1% FAR, EER and rank-1 identification rate are reported in this table. Experiments with WLBP yields better results than raw pixel intensity for subspace modeling and pose correction also helps to greatly improve the performance on both raw pixel intensity and WLBP. The three subspace modeling methods have consistent ranking in terms of rank-1 identification rate performance and from high to low, the ranking is: (1) WLBP with pose correction, (2) WLBP without pose correction, (3) raw pixel with pose correction, and (4) raw pixel without pose correction. Among the three subspace modeling methods, UDP has significantly outperformed PCA by reaching 100% rank-1 identification rate and 98% VR at 0.1% FAR.

As mentioned in Section 3.6, UDP adopts KNN to formulate the scatter matrix and then tries to find the optimal projection that minimizes local scatter matrix S_L and maximizes non-local scatter matrix S_N simultaneously. UDP takes both holistic and local information into account while PCA only considers holistic information and LPP only utilizes local information. That partially explains why UDP yields better results than PCA and LPP. In addition, UDP can learn the spatial information of each input image provided by WLBP and cluster more accurately.

Figure 6 shows the CMC and ROC curves of the experiments both with and without pose correction. Table 2 shows a comparison of age invariant face recognition methods from the literature. Our proposed method is able to reach 100% rank-1 identification rate, a 52.2% increase from by far the best performing result of 47.5% on full face [13]. In addition, we show robustness of WLBP by directly matching the features without subspace modeling and still gain 41.22% rank-1 identification rate on entire FG-NET.

6. Conclusions and Future Work

In this work, we have shown an improved feature extraction approach on periocular region only on age invariant face recognition problem. Following our proposed approach, with all the preprocessing steps, the WLBP featured periocular images with subspace modeling using UDP was able to obtain 100% rank-1 identification rate and 98% VR at 0.1% FAR, a giant leap from by far the best performing algorithm on full face for age invariant face recognition on FG-NET database. Compared to traditional ways of subspace modeling, out novel subspace modeling method has gained significant improvement by building subspaces on WLBP featured image, not on raw pixel intensity. In future we will explore further subspace analysis and other face aging database.

7. Acknowledgment

This research was supported in part by CyLab at Carnegie Mellon University under grants DAAD19-02-1-

Table 2. Comparison of age invariant face recognition methods on FG-NET database [13].

	Approach	(# subjects, # images) in probe and gallery	Rank-1 Identification Rate
Geng *et al*. (2007) [5]	Learn aging pattern on concatenated PCA coefficients of shape and texture from full face across a series of ages	FG-NET (10,10)	38.1%
Park *et al*. (2010) [17]	Learn aging pattern based on PCA coefficients from full face in separate 3D shape and texture spaces from the given 2D database	FG-NET (82,1002)	37.4%
Li *et al*. (2011) [13]	Use multi-feature discriminative analysis (MFDA) method with densely sampled local descriptors (SIFT, MLBP) from full face	FG-NET (82,1002)	47.5%
Proposed method	Apply robust feature extractor WLBP on periocular region only and use UDP to model the subspaces	FG-NET (82,1002)	100%

0389 and W911NF-09-1-0273 from the Army Research Office. One of the authors Felix Juefei-Xu would like to thank Dr. Gao Zheng from Shanghai Jiao Tong University School of Medicine for his plastic surgery related discussions.

References

[1] K. Beauchamp. Applications of walsh and related functions. In *Academic Press*, 1984.

[2] T. Cootes, G. Edwards, and C. Taylor. Active appearance models. *the IEEE TPAMI*, 23:681–685, 2001.

[3] A. Drygajlo, W. Li, and K. Zhu. Q-stack aging model for face verification. In *17th European Signal Processing Conf.*, 2009.

[4] Y. Fu and T. Huang. Human age estimation with regression on discriminative aging manifold. In *IEEE Trans. on Multimedia*, volume 10, pages 578–584, 2008.

[5] X. Geng, Z. Zhou, and K. Smith-Miles. Automatic age estimation based on facial aging patterns. *IEEE TPAMI*, 29:2234–2240, 2007.

[6] R. Gross and V. Brajovic. An image preprocessing algorithm for illumination invariant face recognition. In *4th Int'l Conf. on Audio- and Video-Based Biometric Person Authentication*, pages 10–18, 2003.

[7] G. Guo, Y. Fu, C. Dyer, and T. .Huang. Image-based human age estimation by manifold learning and locally adjusted robust regression. In *IEEE Trans. on Image Processing*, pages 1178–1188, 2008.

[8] X. He and P. Niyogi. Locality preserving projections. In *In Advances in Neural Information Processing Systems 16*. MIT Press, 2003.

[9] F. Juefei-Xu, M. Cha, J. Heyman, S. Venugopalan, R. Abiantun, and M. Savvides. Robust local binary pattern feature sets for periocular biometric identification. In *Fourth IEEE Int'l Conf. on Biometrics: Theory Applications and Systems (BTAS)*, 2010.

[10] F. Juefei-Xu, M. Cha, M. Savvides, S. Bedros, and J. Trojanova. Robust periocular biometric recognition using multilevel fusion of various local feature extraction techniques. In *Proc. DSP2011, 17th Int'l Conf. on Digital Signal Processing*, 2011.

[11] Y. Kwon and N. Lobo. Locating facial features for age classification. In *the Int'l Society for Optical Engineering*, volume 2055, pages 62–72, 1993.

[12] A. Lanitis, C. Taylor, and T. Cootes. Modeling the process of ageing in face images. In *the Seventh IEEE Int'l Conf. on Computer Vision (ICCV), Kerkyra*, volume 1, pages 131–136, 1999.

[13] Z. Li, U. Park, and A. Jain. A discriminative model for age invariant face recognition. In *IEEE Trans. on Information Forensics and Security*, 2011.

[14] G. Mahalingam and C. Kambhamettu. Age invariant face recognition using graph matching. In *Fourth IEEE Int'l Conf. on Biometrics: Theory Applications and Systems (BTAS)*, 2010.

[15] E. Masoro and S. Austad. *Handbook of the Biology of Aging, Seventh Edition*. Academic Press, 2010.

[16] T. Ojala, M. Pietikäinen, and D. Harwood. A comparative study of texture measures with classification based on feature distributions. In *Pattern Recognition*, volume 29, pages 51–59, 1996.

[17] U. Park, Y. Tong, and A. Jain. Age-invariant face recognition. *IEEE TPAMI*, 32:947–954, 2010.

[18] M. Petrou and P. Sevilla. *Dealing with Texture*. Wiley, 2006.

[19] A. Sethuram, E. Patterson, K. Ricanek, and A. Rawls. Improvements and performance evaluation concerning synthetic age progression and face recognition affected by adult aging. In *the 3rd IEEE Int'l Conf. on Biometrics*, 2009.

[20] K. Taylor. *Forensic Art and Illustration*. CRC Press, Boca Raton, 2008.

[21] S. Yan, X. Zhou, M. Liu, M. Hasegawa-Johnson, and T. Huang. Regression from patch-kernel. In *IEEE Conf. on Computer Vision and Pattern Recognition (CVPR)*, pages 1–8, 2008.

[22] J. Yang, D. Zhang, J. Yang, , and B. Niu. Globally maximizing, locally minimizing: Unsupervised discriminant projection with applications to face and palm biometrics. *IEEE TPAMI*, 29:650–664, 2007.